IEEE Access
Multidisciplinary ⋮ Rapid Review ⋮ Open Access Journal

Received 30 October 2023, accepted 17 November 2023, date of publication 21 November 2023,
date of current version 4 December 2023.

Digital Object Identifier 10.1109/ACCESS.2023.3335607

RESEARCH ARTICLE

A Knowledge-Based Multi-Scale Adaptive Classification Approach for Mobile Laser Scanning Point Clouds in Urban Scenes

MINGXUE ZHENG, XIANGCHENG SHEN, ZHIQING LUO, PINGTING CHEN, BO GUAN, JICHENG YI, AND HAIRONG MA

Institute of Agricultural Economy and Technology, Hubei Academy of Agricultural Sciences, Wuhan 430064, China

Corresponding author: Hairong Ma (mahairong1008@126.com)

This work was supported in part by the National Natural Science Foundation of China under Grant 42201397, and in part by the Youth Fund of Hubei Academy of Agricultural Sciences under Grant 2022NKYJJ18.

ABSTRACT With the quick development of mobile light detection and ranging (LiDAR) systems, point clouds are frequently applied for various large-scale outdoor scenes. It is fundamental to quickly and accurately classify objects of mobile laser scanning (MLS) point clouds in such urban scene applications. However, an important problem is the need for massive training samples in object classification. High computational cost is also a common challenge. To overcome them, a knowledge-based multi-scale adaptive classification approach (KMAC) is proposed in the paper. The method consisting of four layers derives from a normal neural network framework, the operation in part layers differ. As the scale difference of various objects in natural environment, 3D multi-scale spatial local relation of objects is explored with inspiration by the idea of convolution. Two types of distinguishable features of actual objects are explored to describe 3D point clouds by a 2D vector representation. Then, human knowledge is used to directly build an end-to-end match between these feature descriptions in 2D and 3D point clouds of actual objects. Point clouds which are adjacent with the same feature representation would be intentionally integrated into multiple adaptive regions. The adaptive integration solves scale difference of various objects. The direct match by knowledge exactly plays the role of training samples. Qualitative and quantitative experimental results on three data-sets finally show the proposed approach is promising to efficiently classify unlabeled objects in urban scenes.

INDEX TERMS Geometrical Eigen-features, adaptive, multi-scale, knowledge, classification, MLS point cloud, urban scene, transfer learning.

I. INTRODUCTION

With the quick development of LiDAR systems, point clouds as a new data source, play an increasingly important role in various urban scene applications [1], [2], [3], [4], [5], [6], such as large-scale urban 3D point cloud classification [1], vehicle detection [2], and road facilities recognition [3]. In many research fields, classification and optimal performance are necessary prerequisites [7], [8], [9], [10], [11]. Especially, for 3D point cloud applications, quick and accurate automated classification procedures for mobile point clouds in complex urban environments are fundamental and highly necessary. Classification of MLS point clouds, in which each point is determined to belong to a specific class, e.g., ground, road, vehicles, and street trees, and so on, is a common and core task for various applications of 3D urban scene analysis [12], [13], [14], [15], [16], [17], [18], [19].

Recently, many scholars have carried out in-depth research and made some progress in the field of classification for MLS point clouds in urban scenes [20], [21], [22], [23], [24], [25], [26], [27], [28], [29], [30], [31], [32], [33], [34]. For example, Aijazi et al. realized the complex task of classification of 3D urban point clouds by combining two approaches, that is, image converting and the super voxel employing [20].

The associate editor coordinating the review of this manuscript and approving it for publication was Nazar Zaki.

Babahajiani et al. identified each type of objects step by step, such strategy could significantly reduce the need for manually labeled training samples [22]. Combining with a support vector machine (SVM) classifier, Li et al. built an object-oriented decision tree to reduce wrong classification and significantly increase the classification accuracy [30]. Li et al. focused on point-wise classification by applying a binary classifier involving a set of local features derived from the neighborhoods of the point [32]. Convolutional neural network-based (CNN) methods also have rapidly began to occupy more than half of related publications in recent years [35], [36], [37], [38], [39], [40], [41], [42], [43], [44], [45], [46], [47]. For example, Huang et al. introduced a framework of 3D CNN and applied for labeling complex 3D point could data in outdoor environment during the voxelization, training and testing of the 3D network [36]. Thomas et al. designed a new kernel point convolution, which consisted of several advantages, including to use any number of kernel points. The approach made it possible to process more complex classification tasks in outdoor scenes [40]. Tan et al. proposed MSTGNet with a revised structure to make comparative performance with state-of-the-art deep learning semantic segmentation methods in a large-scale point-wise labeled urban outdoor point cloud data-set [44]. Network-based models also performed on other classification applications [48], [49], [50], [51], [52], [53], [54].

Lots of high quality classification results are achieved from the above publications, but all these methods depend on supervised learning. It is easy to get high classification performance at the cost of massive labeled samples, lots of parameter setting and heavy computation cost. However, most point clouds collected by mobile LiDAR equipment are raw without label information. Recently open and free data-sets of point clouds are manually labeled, which is labor-intensive and time-consuming. In addition, the common challenges of point classification from MLS point clouds also include a low distinctiveness of local geometric features and a high computational complexity of the neighbor search. Multiple neighborhood scales or a selected optimal neighborhood scale [55], [56], [57], [58], [59] are recovered to enhance the discrimination of local geometric features, resulting in higher computational cost.

In response to the above problems, the following solutions provide good inspiration.

(1) Knowledge-based approaches can be employed, which explore discriminating features of objects based on understanding of the surrounding environment. Therefore, massive training samples are not needed.

(2) To enhance the robustness of methods, it is critical to exploit discriminating characteristics of urban objects which are not easily affected by the external environment. Geometric features, which are reflected by several closely spaced points, have always been considered for discriminating feature extraction. Furthermore, knowledge-based approaches can help to realize the extraction of geometric features.

(3) The knowledge-based approach can save lots of computation time with no heavy training process.

Actually, from the early 90s, many researchers were always working to reduce the need for training samples [60], [61], [62]. Recently, the line of research is active again [63], [64], [65]. Zheng et al. implemented vehicle recognition based on region growth of relative tension and similarity measurement of side projection profile of vehicle body in urban scenarios [65]. Some research about small amount of samples in classification also are working [66], [67]. For example, Zhao et al. [66] proposed a method for point cloud classification based on transfer learning using small training data-sets. These work easily result in the over-fitting problem when the numbers of training samples are relatively small.

Based on above overview, a knowledge-based multi-scale adaptive classification method (KMAC) on urban objects for unlabeled point cloud data-sets is proposed in the paper. The KMAC method is derived from a normal neural network framework, and borrows classic idea in each layer of the latter. The former replaces the need for training samples by incorporating human knowledge. The idea of multi-scale is first used to partition point cloud data in 3D space. Then relevant features per region are extracted including height difference and geometrical eigen-feature. Screening by first law of geography, these neighborhoods within point clouds which are with similar characteristics are selected out to shape 3D adaptive spatial regions. Finally, human knowledge on real objects is used to build a direct classification match between the extracted features and the classes of real objects.

The paper is to solve the classification problem without label information. The aim of this paper is to look for a feasible method for both feature extraction and point cloud classification based on knowledge to efficiently classify unlabeled urban objects. Inspiring by classic principle in each layer of a normal neural network framework, multi-scale partition, relevant feature extraction, 3D adaptive spatial region forming, and knowledge-driven classification are involved into each layer of the KMAC method, finally to efficiently classify unlabeled urban objects. The proposed method provides ideas and guidance for the classification of unlabeled objects in urban scenes.

The novelty of the work is that:

(1) In view of the difficulty of the scale difference of urban objects, the idea of adaptive integration for 3D spatial regions is proposed, which takes full account of the multi-scale characteristics of urban objects.

(2) Knowledge rules on urban objects play the role of a classifier, which satisfies the classification requirement without label information. It reduces the complexity of the problem and saving computing resources.

Fig. 1 illustrates the proposed workflow. The core of the proposed workflow is KMAC, which is on the base of four modules of a normal CNN consisting of input layer, convolutional layer, fully connect layer, and output layer. At the input layer, data preprocessing is necessary, of which details

are given in Section II-C-I. Then, the remaining points are fed to the convolutional layer of the proposed KMAC method. Distinctive properties of objects in natural environment are hardly defined at a unique scale. In order to overcome the difficulty, the multi-scale spatial relation of objects is analyzed in four steps inspiring by the idea of convolution in a normal CNN. The details are presented in Section II-C-II. At the convolutional layer, based on human knowledge, two types of discriminating features of objects are extracted. 3D adaptive spatial regions for objects are captured in fully connected layer in Section II-C-III. The final output in the pine-line of KMAC method is classified point clouds in Section II-C-IV. Finally, to verify the robustness and extensibility of the proposed method, the KMAC method is tested on unlabeled point cloud data-set by the concept of transfer learning.

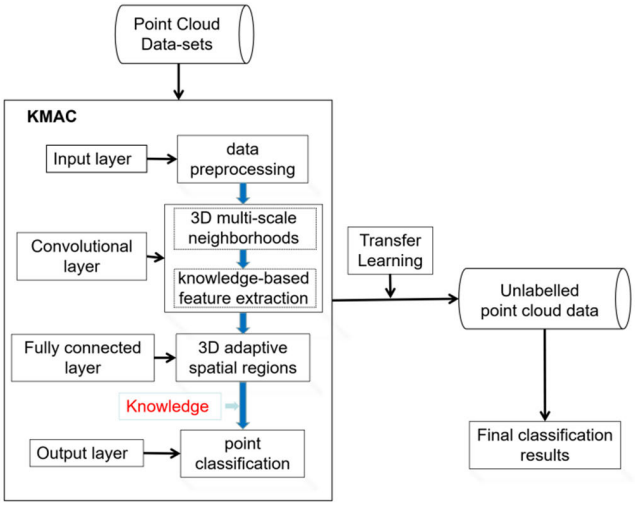

FIGURE 1. The proposed workflow.

Three main contributions of the work in the paper include:

(1) Based on human knowledge, the proposed KMAC method is without the need of massive training samples. This greatly reduces the pressure to produce training labels by humans. And it can save lots of computation time with no heavy training process.

(2) The KMAC approach can integrate adaptive spatial regions to solve scale difference of various objects. According to the first law of geography, the construction of 3D adaptive spatial region is implemented. The adaptive output solves scale difference of various objects. Direct classification match also avoids the time-consuming training process.

(3) For a comfortable life environment, basic pattern of artificial objects in public places is similar in different cities and countries. The similarity makes the proposed KMAC method suitable for various urban scenes by transfer learning.

The remainder of this paper is organized as follows. Section II introduces the proposed method. Section III presents the experiment results, Section IV gives the discussion, and Section V presents the conclusion.

II. METHODOLOGY

The aim of this paper is to look for a feasible method for both feature extraction and point cloud classification based on knowledge to efficiently classify unlabeled urban objects, rather than pursuing perfect classification accuracy from labeled MLS point clouds.

In Section II-A, class defining depending on experiment data-sets is given. In Section II-B, a simple introduction of a normal CNN is presented. Then the individual layers of the proposed KMAC method in Fig. 1 are explained to complete a whole procedure of urban object classification in Section II-C. In the final section II-D, three common measure criteria are described to evaluate the proposed method.

A. CLASS DEFINING

The class type of urban objects directly impacts on the design of a classification method. It is necessary to initially define classes. The data-sets selected in the paper include two mobile laser scanning benchmarks in different districts in Paris, France [68], [69], and another one from a company called Cyclomedia, which mainly covers city scenes in Schiedam, Netherlands. Considering the variety of types of objects in these three urban scenes, and the proportion of each type of object, four classes (i.e., Facade, Trees, Ground and Others) are defined in the paper.

B. THE ARCHITECTURE OF A NORMAL CNN

A simple CNN as shown in Fig. 2 generally consists of four layers, that is, one input layer, one output layer, one convolutional layer and one fully connected layer.

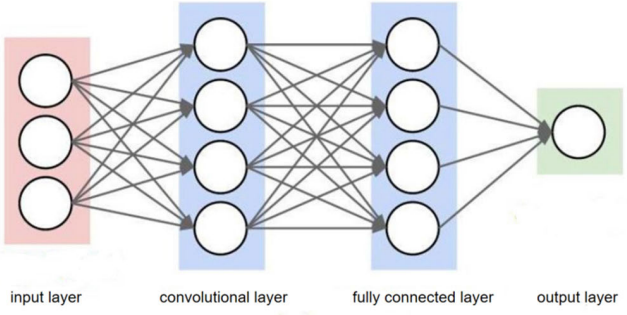

FIGURE 2. A simple CNN architecture.

It is easy to understand the function of input and output layers. The convolutional layer is the core module of a normal CNN. Its objective is to extract valuable features from input data. Four hyper-parameters control output of a convolutional layer, that is, the depth, stride, the filter size, and zero-padding as shown in Table 1. A fully connected layer is to learn combinations of the valuable features. Inspired by a typical CNN, the knowledge-based multi-scale adaptive classification method is presented in next section.

TABLE 1. Four main hyper-parameters in a convolutional layer and the individual description.

Hyper-parameter	Symbol	Description
depth	K	corresponding to the number of filters.
stride	S	with the stride to slide the filter.
spatial extent	F	deciding the local size of convolution each time.
zero-padding	P	allowing to control the spatial size of the output.

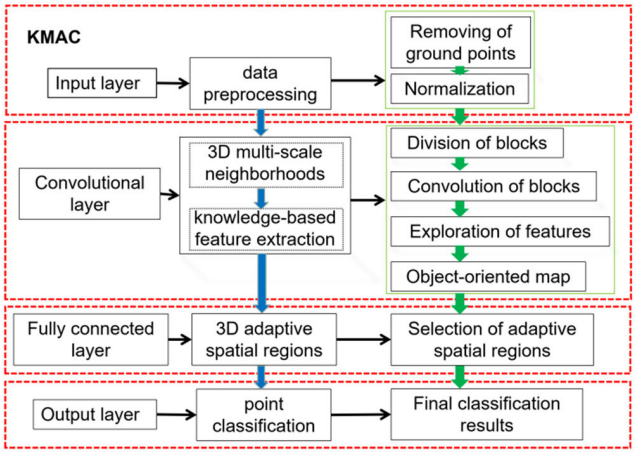

FIGURE 3. KMAC.

C. KNOWLEDGE-BASED MULTI-SCALE ADAPTIVE CLASSIFICATION (KMAC)

A knowledge-based multi-scale adaptive classification method (KMAC) on urban objects for unlabeled point cloud data-sets is proposed in the paper. KMAC consists of four layers as shown in Fig. 3. Details are given in following subsections.

1) INPUT LAYER OF THE KMAC

Data preprocessing is performed in the input layer. The ground points are removed by the software CloudCompare [70], [71], [72]. Many features for point clouds, for example, point density, depend on the distance from the sensor and the velocity of the car on which the laser scanners are mounted. The further away from the sensor, the coarse the point density. To make the proposed method insensitive to such features, these features should be scale invariant. Normalization is used in the paper. The process is shown in Fig. 4. Whole point clouds are separated into lots of small same-sized cubes in Fig. 4(a). In Fig. 4(b), the number of point clouds differs in each cube because of point density. In Fig. 4(c), only one point is reserved and all other points are removed in each regular cube. The selected point is close to the red centre point of the small cube. There are two benefits for normalization:

1) ensure the comparability of same feature on different objects.
2) eliminate the adverse effects caused by singular sample data.

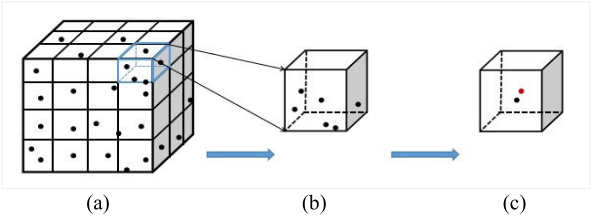

FIGURE 4. Normalization.

2) CONVOLUTIONAL LAYER OF THE KMAC

Generally, the objective of the convolution operation in a normal CNN is to extract valuable features from the input data. The idea of convolution is introduced for feature extraction of unlabeled multi-scale samples and then build an object-oriented map based on knowledge in the KMAC in the section. It is a four-step strategy as shown in Fig. 5. The details in each step are described as follows.

Step I: the division of blocks

Block division aims at separating whole point clouds into a lot of blocks, making sure points in each block belong to the same object as far as possible. Point clouds are divided into 3D blocks through the following process in the paper.

(1) Given the point cloud data-set, the maximum value and minimum value of x, y coordinates on the XOY plane are figured out, forming a plane bounding rectangle of the whole point clouds.

(2) The rectangle is divided into lots of square tiles with the same length.

(3) Adding the z coordinate per point in each tile, the 2D tile is extended to a 3D block. The height value of each 3D block is the z value of the highest point inside the 3D block. Without special explanation, such a 3D block is called a block unit in the paper.

The outputs of the division of blocks are lots of 3D block units. For example, as shown in Step I of Fig. 5, there are $M*N$ 3D gray block units, heights of which differ. M and N is the number of rows and columns of these 3D gray block units, respectively on the XOY plane. The height difference among 3D block units exactly reflects the height characteristics of ground objects.

Based on the results of block division, multi-scale neighborhood areas consisting of 3D block unites will be integrated by convolution in next step.

Step II: the convolution of blocks

Block convolution aims at searching for multi-scale neighborhood areas for objects, further preparing for feature extraction in each area in the paper.

Distinctive properties of objects in natural environment are hardly defined at a unique scale. The scale even could

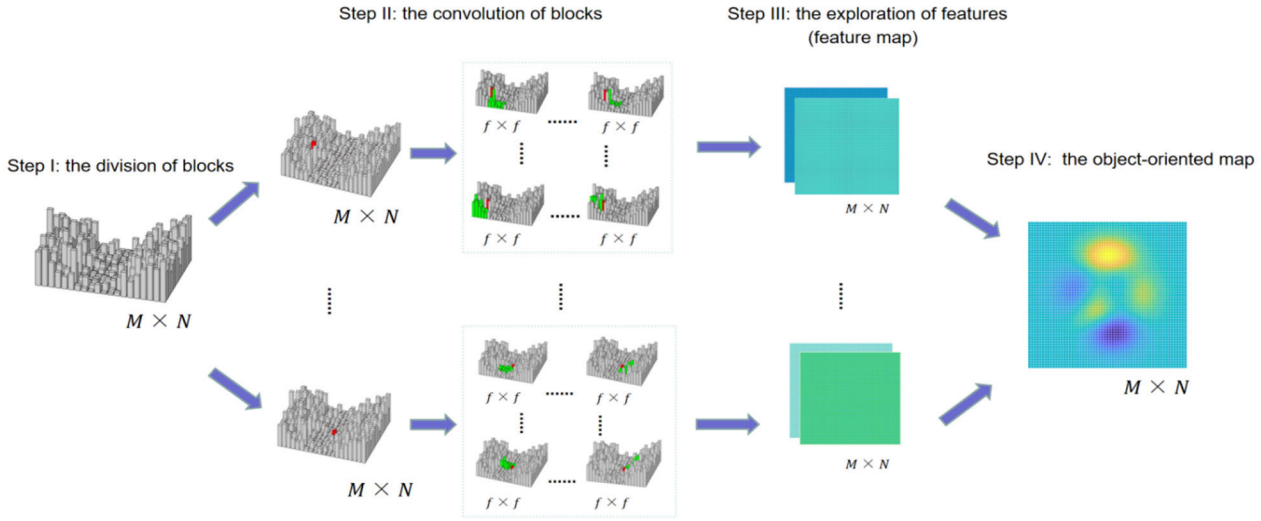

FIGURE 5. The four-step strategy in the convolutional layer of the KMAC.

be different among objects in the same class. To overcome the difficulty, block convolution is proposed to explore multi-scale spatial information of objects.

Take a $f \times f$ ($f \geq 1$) filter as the example, block units of number f^2 are convoluted at a time. These block units are stored as one neighborhood area, which covers these f^2 blocks and points inside them. With the filter sliding, lots of such areas with block units of number f^2 can be gotten.

The outputs of the convolution of blocks are lots of neighborhood areas. For example, as shown in Step II of Fig. 5, the 3D block unit in red is the considering block, 3D block units in green are its neighborhood blocks, the number of which in green is $f^2 - 1$. The $f \times f$ filter slides around the red block from left-right and top-down. Generally there are f^2 such neighbourhood areas containing the 3D red block unit when the stride S is 1. In Step I, the length and width of each block unit are clear. Number f changes, a series of spatial extend F are easy to be gotten. Spatial extend F exactly embodies the concept of multi-scale.

Based on the results of block convolution, two types of features will be extracted from point clouds of neighborhood areas in step III.

Step III: the exploration of features

Considering class type of urban objects without label information in experimental data-sets, traditional knowledge-based features are considerable. Two types of features are explored in the paper, e.g., height difference and geometrical eigen-features of objects. The depth K is the number of types of extracted features, and the depth is 2 in the paper.

a: HEIGHT DIFFERENCE

Height difference, Δh, is the distance of the z coordinate between the lowest and highest points inside a block unit. A 3D block unit, presents a low height difference if points inside it belong to ground points. Otherwise it shows a large height difference if vertical objects are inside it, including facades or trees.

b: GEOMETRICAL EIGEN-FEATURE

Normally, the linearity feature can be used to detect line structures, the planarity feature has the ability to discriminate planar structures, and the scattering feature allows the exhibition of 3D structures [73], [74]. With the results of the division of blocks in Step II, three geometrical eigen-features (e.g., linearity l_λ, planarity p_λ, and scattering s_λ) are defined to identify the shape of points in each 3D neighborhood area. Details are given below [75].

Given a 3D point set $P_{set} = \{p_i = (x_i, y_i, z_i) | i = 1, 2, \ldots, n\}$ within a region, an efficient method to compute and analyze the 3D point set P_{set} is to diagonalize the covariance matrix of P_{set}. In a matrix form, the covariance matrix of P_{set} is written as

$$C(P_{set}) = \frac{\sum_{p_i \in P_{set}} w_i (p_i - \bar{p})^T (p_i - \bar{p})}{\sum_i w_i} \tag{1}$$

where $\bar{p}$ represents the mean of the points, that is,

$$\bar{p} = \frac{1}{n} \sum_{i=1}^{n} p_i \tag{2}$$

and n represents the number of points in P_{set}. w_i is weight of point p_i, generally $w_i = 1$. The eigenvectors and eigenvalues of the covariance matrix are computed by using a matrix diagonalization technique, that is, $V^{-1}CV = D$, where D is a diagonal matrix containing the eigenvalues, i.e., $\lambda_1, \lambda_2, \lambda_3$ of C. V is an orthogonal matrix that contains the corresponding eigenvectors. The obtained eigenvalues are greater than or equal to zero, that is $\lambda_1 \geq \lambda_2 \geq \lambda_3 \geq 0$. It is worth noting that the occurrence of eigenvalues identical to zero must be avoided by adding an infinitesimal small value. Situation $\lambda_1 \geq \lambda_2, \lambda_3$ represents a stick-like ellipsoid, meaning a linear

structure. Situation $\lambda_1 \approx \lambda_2 \geq \lambda_3$ indicates a flat ellipsoid, representing a planar structure. Situation $\lambda_1 \approx \lambda_2 \approx \lambda_3$ corresponds to a volumetric structure.

Based on the geometrical property, three geometrical eigen-features are defined [75]. Here the definitions of the eigen-features of linearity l_λ, planarity p_λ, and sphericity s_λ are given as follows:

$$l_\lambda = (\lambda_1 - \lambda_2)/\lambda_1 \quad (3)$$

$$p_\lambda = (\lambda_2 - \lambda_3)/\lambda_1 \quad (4)$$

$$s_\lambda = \lambda_3/\lambda_1 \quad (5)$$

where $l_\lambda + p_\lambda + s_\lambda = 1$.

Based on above, height difference and geometrical eigen-features of 3D point clouds are extracted from every neighborhood area with f^2 block units. For each block unit in such one neighborhood area, the value of height difference is different but those of geometrical eigen-features are shared.

With the stride S being 1, it is sure a block unit appears in multiple neighborhood areas, feature characteristics reflected by these areas probably differ. In the case, the rule of vote is applied to select the most suitable characteristics for every block unit. For example, the 3D block unit in red is the considering block in Step II of Fig. 5. There are f^2 such neighbourhood areas containing the 3D red block unit when the stride S is 1. Geometrical eigen-features of number f^2 in these neighbourhood areas are obtained, and only one is selected out to describe the 3D red block by voting. If a block unit appears in nine areas, where shape structure of points respectively present linearity of number two, planarity of number three, and sphericity of number four. Then sphericity structure is assigned to the block unit and point clouds inside it.

The outputs of the exploration of features are feature maps based on extracted features. For example, as shown in Step III of Fig. 5, each rectangle is a feature map, which reflects one characteristic of objects. The size of feature maps is $M \times N$, and the types of feature map contain height difference-based and geometrical eigen-feature-based. The element in each grid of a feature map presents feature value of point clouds in every 3D block unit. The number of the feature map of objects equals to the number of the type of features extracted.

Based on the results of the exploration of features, an object-oriented map will be built in next step.

Step IV: the object-oriented map

In the step, an object-oriented map based on knowledge for classification in urban scenes is built. As described in step III, the type of feature map contains height difference-based and geometrical eigen-feature-based. The element in each grid of a feature map presents feature value of point clouds in every 3D block unit. By integrating two feature maps into one, every 3D block unit refers to a 2D vector representation. Each 2D vector is the feature combination of height difference and geometrical eigen-feature. All 3D block units are transferred into a object-oriented map by 2D vectors. As shown in Step IV of Fig. 5, those block units referring to the same vector representation are coloured in the same color, and different vector representations correspond to different colors. The color distribution on the map is object-oriented. Adjacent areas are mostly in the same color.

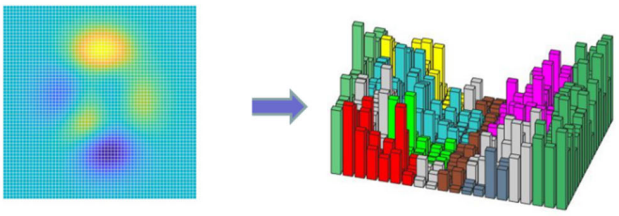

FIGURE 6. Adaptive spatial regions for various objects in 3D space. (a) an object-oriented map in 2D space; (b) adaptive spatial regions in 3 space,different regions in different colors.

3) FULLY CONNECTED LAYER OF THE KMAC

In the proposed KMAC method, this layer aims at forming adaptive spatial regions for various objects by the object-oriented map. In the process, each adaptive spatial region is formed by the nearest blocks, which conforms to the first law of geography [76]. The first law of geography states that "everything is related to everything else, but near things are more related than distant things."

As described in section II-C-II, after the convolutional layer of KMAC method, point clouds in each 3D block is mathematically presented by a 2D vector. An object-oriented map in 2D space is transferred to integrate spatial regions in 3D space. These 3D block units, which are adjacent with the same vector representation would be integrated into one new region. Then, adaptive spatial regions for various objects in 3D are shaped.

As shown in Fig. 6, adaptive spatial regions in different colors are visualized. Fig. 6(a) shows an object-oriented map in 2D space, and Fig. 6(b) shows adaptive spatial regions in 3D space, different regions are displayed in different colors.

4) OUTPUT LAYER OF THE KMAC

The output in this layer is that each point is assigned to a class, which exactly is the class of an adaptive spatial region where the point is located.

Based on 2D vector representation of feature combination for point clouds in 3D blocks, made-up labels in terms of extracted features for classifying the objects are introduced [72]. The base of made-up labeling is the knowledge, that is, human understanding on the extracted features. Simply speaking, every 3D block is given a made-up label based on height difference of point clouds inside it. Three eigen-features of point clouds inside the 3D block is used to generate another made-up label. As a result, the 3D block is presented by a 2D vector representation of the combination of these two made-up labels. Human knowledge on real objects is used to build a direct end-to-end match between the combinations of made-up labels and the classes of real

objects. The core behind the point cloud classification is the knowledge. For example, both facades and trees belong to height objects in urban scenes (given made-up label a_1). There are differences in physical structure for them. Class Facade presents a planar structure (given made-up label b_1), class Trees presents a volumetric structure (given made-up label b_2). Based on knowledge on these two defined classes, an end-to-end match between class Facade and 2D made-up label $[a_1, b_1]$ is built. Also, an end-to-end match between class Trees and 2D made-up label $[a_1, b_2]$ is built. The same to class Ground and class Others.

So far, the knowledge-based multi-scale adaptive classification process for unlabeled MLS point clouds in urban scenes is fully implemented. Although the architecture of a normal CNN is borrowed, it does not include sample training in the complete process. Classes are assigned to points based on human knowledge of feature combinations [72]. This classification method, similar to a classifier, plays the role of training samples. The proposed method could provide feasible ideas and guidance for the classification of unlabeled objects in urban scenes.

D. MEASURE CRITERION

In the section, three indexes are employed to evaluate the performance of the KMAC method, respectively, precision, recall and overall accuracy (OA). Those expressions are listed as follows.

Precision (P)- a measure of exactness or quality.

$$P_i = TP/(TP + FP) = F_{i,1,1}/(F_{i,1,1} + F_{i,2,1}) \quad (6)$$

Recall (R)- a measure of completeness or quantity.

$$R_i = TP/(TP + FN) = F_{i,1,1}/(F_{i,1,1} + F_{i,1,2}) \quad (7)$$

Overall accuracy (OA):

$$\begin{aligned} OA_i &= (\mathrm{TP} + \mathrm{TN})/(\mathrm{TP} + \mathrm{FP} + \mathrm{FN} + \mathrm{TN}) \\ &= (F_{i,1,1} + F_{i,2,2})/(F_{i,1,1} + F_{i,1,2} + F_{i,2,1} + F_{i,2,2}) \end{aligned} \quad (8)$$

where four related variables $F_{i,1,1}$,$F_{i,1,2}$,$F_{i,2,1}$ and $F_{i,2,2}$ are listed in Table 2.

TABLE 2. Four common measures.

Measure	Description
$F_{i,1,1}$	true positives (*TP*), point samples in class *i* are assigned to the class *i*.
$F_{i,1,2}$	false negatives (*FN*), point samples in other classes are assigned to the class *i*.
$F_{i,2,1}$	false positives (*FP*), point samples in class *i* are assigned to other classes.
$F_{i,2,2}$	true negatives (*TN*), point samples in other classes are assigned to other classes.

TABLE 3. Four classes and corresponding number of points in the IQmulus and TerraMobilita contest data-set before and after normalization.

Class name	Number before normalization	Number after normalization
Others	540,617	39,274
Facade	7,027,016	438,508
Ground	4,229,639	75,802
Trees	42,039	11,569
Total	**12,000,000**	**604,438**

III. RESULTS

A. EXPERIMENT ON THE IQMULUS AND TERRAMOBILITA CONTEST DATA-SET

1) CLASSIFICATION RESULT

The IQmulus and TerraMobilita Contest data-set [68] contains 3D MLS data from a dense urban environment in Paris. In the paper, all classes in the data-set are limited into four classes, i.e., Facade, Trees, Ground, and Others. Table 3 presents four classes and corresponding number of points before and after normalization. By comparing numbers in the table, 5% of samples are experimented.

Table 4 gives the overall results of the IQmulus and TerraMobilita Contest data-set by the proposed KMAC method. The entry at the $(i+1)$-th row and the $(j+1)$-th column denotes the number of points of the original class of corresponding row that are classified as the class of corresponding column, $i, j = 1, 2, 3, 4$. The OA is 84.94%.

In Table 4, the method performs well for class Facade, Ground and Trees, and performs badly for class Others. 2,376 points of class Others are wrongly classified into class Ground. In the benchmark [68], part points of class Ground are mislabeled as class Others which causes wrong ground truth and misjudgment. Also in Table 4, part points of class Others are wrongly assigned to class Facade. The sub-categories in class Others are various and complex, such as cars and pole-likes. These sub-categories are close to class Facade, causing the disturbance for classification. The performance should be improved by dividing class Others into finer sub-categories as provided in the benchmark and extracting more distinguishable features for classification.

TABLE 4. Classification results of the IQmulus and TerraMobilita contest data-set by the KMAC.

class name	Others	Facade	Ground	Trees	Precision
Others	17,938	3,124	2,376	289	0.7560
Facade	24,323	378,330	9,893	25,962	0.8628
Ground	6,581	9,985	57,547	1,689	0.7592
Trees	2,201	4,262	364	59,574	0.8972
Recall	0.3514	0.9561	0.8200	0.6807	
OA					**0.8494**

Fig. 7 shows the ground truth and predicted results for each class. Especially, point clouds of class Trees are in green; point clouds of class Ground are in blue; point clouds of class Facade are in gray; point clouds of class Others are in red. For these four classes, point clouds which are wrongly classified are in purple. From the results, although having no training process, the generated results show distinguished classification effect for different objects. However, there are still some errors for four classes.

In Fig. 7(b), some ground points close to facades are wrongly classified as facade points. Inversely, some non-ground points close to ground are wrongly classified as ground points in Fig. 7(d). In the benchmark, the sub-categories in class Others are complex, such as cars and pole-likes. In Fig. 7(f), those point clouds that are not clearly characterized in the proposed KMAC method are wrongly classified as class Others. In Fig. 7(h), point clouds in purple belong to the attachments of facades. Two types of features (height difference and geometrical eigen-features) between the attachments of facades and trees are represented similarly in Step III of the KMAC, which causes a classification error. More fine features need to be explored to improve classification accuracy between the attachments of facades and trees. Fig. 8 shows the complete ground truth and final classification results by the proposed method for four classes.

2) COMPUTATION TIME

The algorithm runs on a computer with Intel(R) Core(TM) I7-7700HQ CPU @ 2.80 234 GHz with 4 cores, RAM 16.0 GB. The programming language is in MATLAB. The core cost of computation time in the proposed KMAC method is in convolutional layer and fully connected layer, that is, the shape of adaptive spatial regions. Concerning the computational complexity, the computation time required for processing different numbers of point clouds is considered. Compared to the proposed method on processing point cloud segmentation, three highly relevant algorithms DBCSAN [77], k-means [78], mean shift [79] are elaborated below.

DBSCAN model uses a simple minimum density level estimation, based on a threshold for the number of neighbors within the radius. It consists of three major contributions: (1) the model can cluster dense data-sets of any shape; (2) the model is not sensitive to outliers in the data-set; (3) there is no bias in the clustering results. Clustering effect of the model is very sensitive to parameters. If the sample set is large, the convergence time is a great challenge.

K-means is the most popular clustering algorithm based on Euclidean distance. The basic idea of k-means is that the closer the distance between two objects, the greater the similarity. K-means is simple in principle and has only one parameter. However, the model is sensitive to outliers and noise. The convergence speed is affected in 3D space. In addition, only globular clusters can be found by k-means model.

Mean shift is a non-parametric estimator of density gradient, which is employed in the joint, spatial-range (value) domain of gray level and color images for discontinuity preserving filtering and image segmentation. The advantage of mean shift model is fast and robust to target deformation and occlusion. The algorithm lacks the necessary template updates.

TABLE 5. Classification results of the Paris-Rue-Madame data-set by the KMAC.

class name	Others	Facade	Ground	Precision
Others	43618	8555	2900	0.7920
Facade	15330	461921	8983	0.9500
Ground	30356	39432	94688	0.5757
Recall	0.4884	0.9059	0.8885	
OA				**0.8504**

In Fig. 9, it shows the side-by-side computation time comparison of region segmentation among highly relevant algorithms DBCSAN, k-means, mean shift and the proposed KMAC method. To show the computational complexity more clearly, the vertical axis shows the logarithmic value of computation time.

From Fig. 9, it becomes apparent that the mean shift algorithm shows superior computational advantage when increasing numbers of considered point clouds. It is followed closely by the proposed KMAC method. One of the common drawbacks to mean shift algorithm is that it is not suitable for multi-scale objects, which exactly is one of the key considerations in the paper. The computational burden of DBSCAN algorithm is heavier than the proposed method and mean shift algorithm. Three given values in green line in Fig. 9 reflect that required computation time is the most difficult problem when considering k-means algorithm.

B. EXPERIMENT ON THE PARIS-RUE-MADAME DATA-SET

The Paris-Rue-Madame data-set [69] contains 3D mobile laser scanning data from Rue Madame, a street in the 6th Parisian district, France. Table 5 gives the overall results of the Paris-Rue-Madame data-set by the KMAC method. The entry at the $(i+1)$-th row and the $(j+1)$-th column denotes the number of points of the original class of corresponding row that are classified as the class of corresponding column, $i, j = 1, 2, 3$. The OA is 85.04%.

In Table 5, the method performs well for class Facade, and well for class Ground on recall. Part points of class Facade and class Ground are wrongly assigned to class Others. The sub-categories in class Others are various and complex, such as cars and pole-likes. These sub-categories are close to class Facade and class Ground, causing the disturbance for classification. At the same time, these point clouds that are not clearly characterized in the proposed KMAC method are wrongly classified as class Others. The performance should be improved by dividing class Others into finer sub-categories as provided in the benchmark and extracting more distinguishable features for classification.

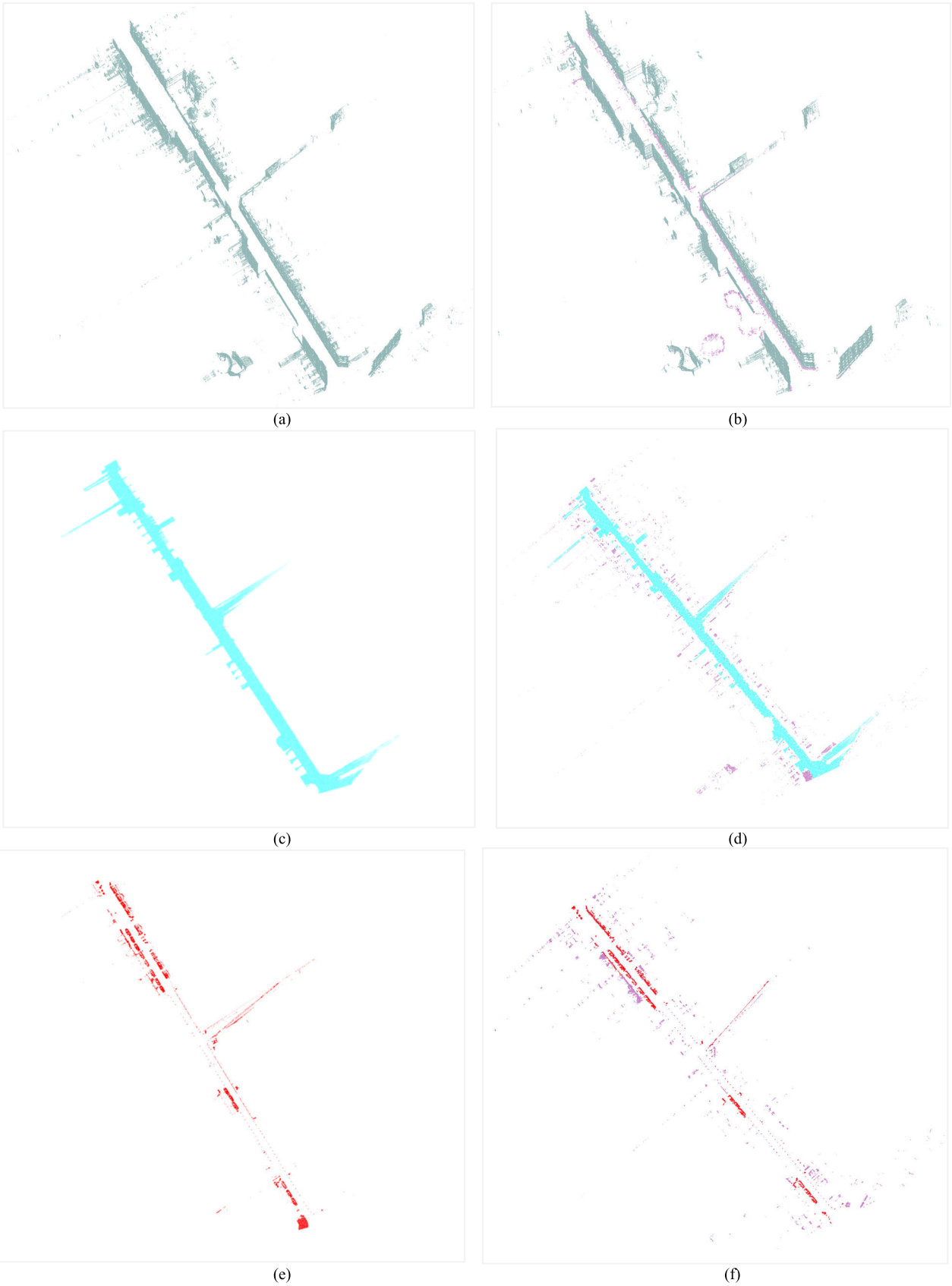

FIGURE 7. Ground truth and predicted result for each class. Ground truth respectively for facade, ground, others, and trees (a, c, e, g). Predicted result respectively for facade, ground, others, and trees (b, d, f, h). (green: class Tree; blue: class Groun; gay: class Facad; red: class Others. purple: error).

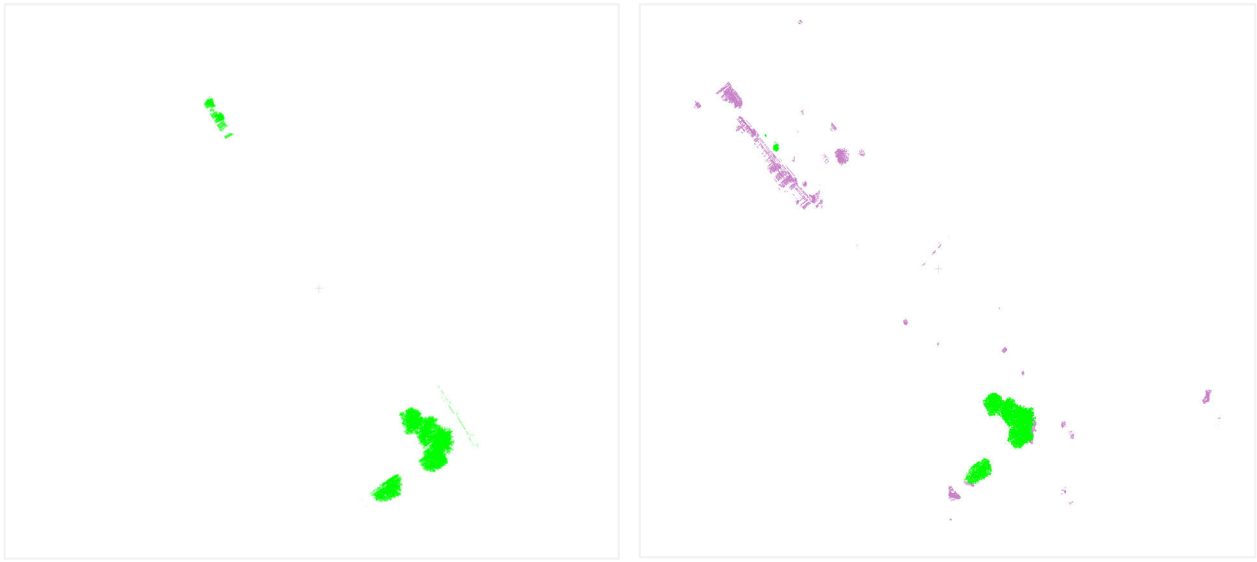

(g) (h)

FIGURE 7. *(Continued.)* **Ground truth and predicted result for each class. Ground truth respectively for facade, ground, others, and trees (a, c, e, g). Predicted result respectively for facade, ground, others, and trees (b, d, f, h). (green: class Tree; blue: class Groun; gay: class Facad; red: class Others. purple: error).**

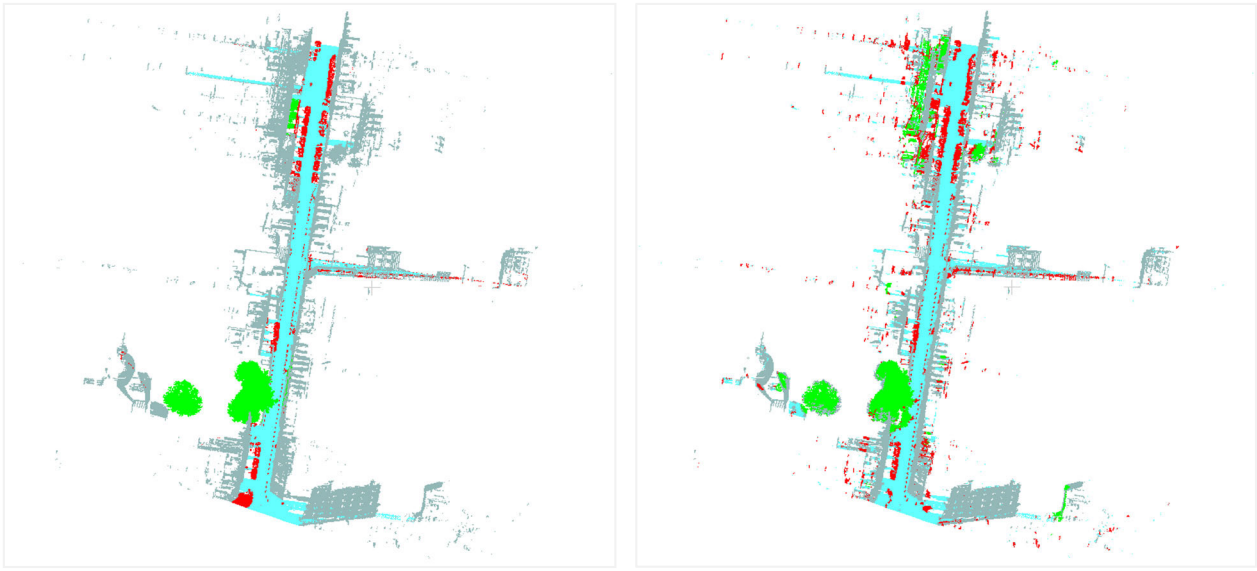

(a) (b)

FIGURE 8. **Ground truth and the final classification result. (a) the ground truth; (b) final classification result. (green: class tree; blue: class groun; gay: class facad; red: class others).**

C. EXPERIMENT ON THE TUDelft CAMPUS DATA-SET

The proposed method is qualitatively tested on the Delft University of Technology (TUDelft) campus data-set which does not contain label information in the section. The TUDelft campus data-set is acquired on March 22, 2016, by the Fugro Drive-Map MLS system.

In 2007, West et al. put forward the concept of transfer learning [80]. The main idea behind transfer learning is to extract important information from some related domains to help to accomplish tasks in the domain of interest [81], [82]. In many applications, it is expensive to collect sufficient training data. It would be more practical if one could reuse the knowledge that is already extracted from some related domains/tasks for use in the domain of interest [83]. Here, the proposed KMAC method in the IQmulus and TerraMobilita Contest data-set is transferred to apply for the TUDelft campus data-set. Fig. 10 shows the original view and final classification result for the TUDelft Campus data-set. In Fig. 10, the proposed KMAC method performs well on the TUDelft campus data-set. Most points which represent

TABLE 6. A comparison with the results in the same data-set [68].

	weinmann et al. [84]		Hackel et al. [55]		the proposed method	
Class name	Recall	Precision	Recall	Precision	Recall	Precision
Facade	0.8721	0.9928	0.9421	0.9964	**0.9561**	0.8628
Ground	0.9646	0.9924	0.9822	0.9871	0.8200	0.7592
Trees	0.8602	0.2566	0.8478	0.5662	0.6807	**0.8972**

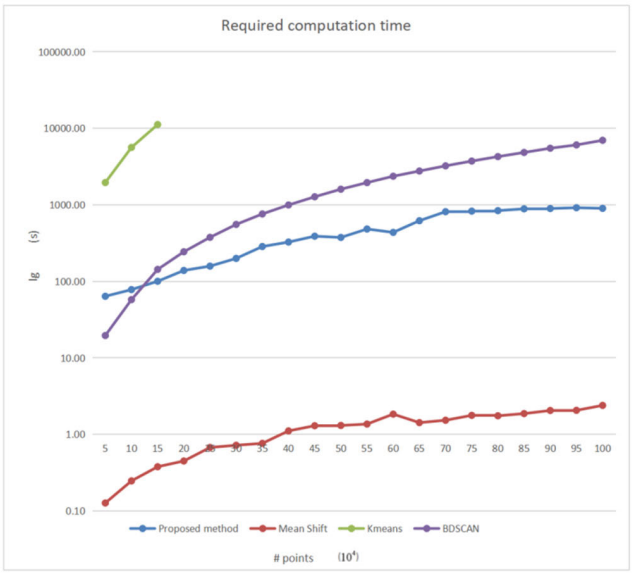

FIGURE 9. The side-by-side computation time comparison of region segmentation among DBCSAN, k-means, mean shift, and the proposed method.

the main structure of facades in gray and trees in green are correctly classified. Most of ground points also are correctly recognized. Part attachments of facades and part of edge points of trees are wrongly assigned to class Others, which would be corrected by refining the proposed method and extracting more valuable features.

The urban environment reasonably exists because it is suitable for human habitation and living. It means that basic patterns of urban objects are similar even in different cities and countries. The commonality makes it possible to apply the proposed KMAC method to various urban scenes.

IV. DISCUSSION

A. COMPARATIVE STUDIES

Table 6 shows a comparison with the results [55], [84] in the same data-set [68]. The results of three same classes Ground, Trees and Facade in these three work are selected out to make the comparison. The results in the table show that the KMAC method performs well expect for class Ground. Combining the ground truth and classification results, a conclusion is drawn. In the proposed KMAC method, features are extracted only depending on human knowledge. The proposed method is sensitive to credibility and completeness of ground truth. Several examples are given as follows.

Incorrect label information among classes on ground truth is a negative factor for object classification. For example, Fig. 11 gives the visualization of part of ground truth. In Fig. 11(a), class Others including ground points is in dark blue, class Trees including ground points is in green. Incorrect label information of class Trees and Others in red boxes easily causes classification error of class Ground.

(2) The completeness of object samples is also an important factor. For example, Fig. 11(b) is top view of part of tree samples on ground truth. The collection of tree samples in the red box is not complete, which affects the performance judgement of geometrical eigen-features.

By correcting and completing ground truth, the proposed KMAC method should perform better. In summary, it does not aim at achieving the best classification accuracy, but to explore a way of both feature extraction and classification for unlabeled samples in the paper. Quantitative results in Table 4, Table 5 and qualitative results in Fig. 10 demonstrate the method is feasible.

Table 7 shows another comparison with the results [84] in the same data-set [69]. By comparison, the proposed method performs excellent on class Facade and near the result value acquired by weinmann et al. Although a lower precision value for class Ground, the proposed method obtains the better recall to classify ground points. Fig. 12 shows the computation time comparison of the proposed method and the existing work by weinmann et al. [84]. In Fig. 12(a), it is done for 3D block division, and in Fig. 12(b), it is done for feature extraction. It becomes apparent that the proposed method presents superior computational advantage for increasing numbers of considered 3D points on both 3D block division and feature extraction. Rather than high classification accuracy, the aim of this paper is to look for a feasible method for both feature extraction and effective classification based on knowledge to classify unlabeled urban objects. Comparative studies demonstrate the proposed method is competitive and promising.

B. PERFORMANCE OF MULTI-SCALE

The idea of convolution is used to explore multi-scale spatial local relation of objects in the paper. As given in Section II, there are four important hyper-parameters in a convolutional layer, that is, the depth, stride, the filter size, and zero-padding.

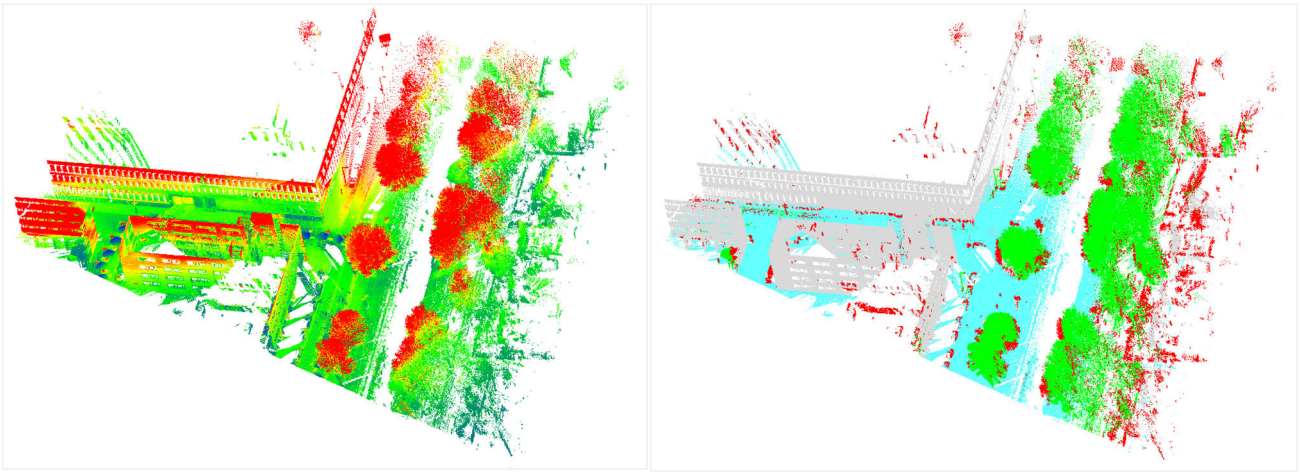

(a) (b)

FIGURE 10. The original point clouds and the final classification result for the TUelft Campus data-set. (a) original scene (Red, green, etc.: different reflectance values of point clouds; (b) the final classification result (green: class Trees; blue: class Groun; gay: class Facad; red: class Others.).

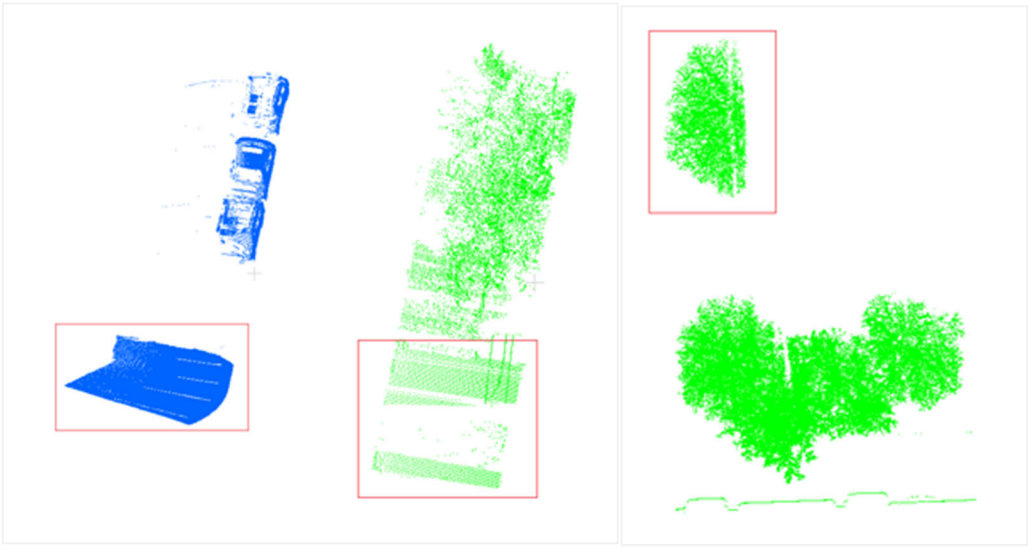

(a) (b)

FIGURE 11. The visualization of part of ground truth. (In box retangle, green: class Trees; blue: class Ground).

TABLE 7. A comparison with the results in the same data-set [69].

	weinmann et al. [84]		the proposed method	
Class name	Recall	Precision	Recall	Precision
Facade	0.953	0.962	0.906	0.950
Ground	0.865	0.978	**0.889**	0.571

In the paper, the depth is the number of types of extracted features, that is, $K = 2$. Real input data is directly used instead of padding border with zeros, that is, $P = 0$. As 5% of samples are tested because of normalization, stride S is set as 1 to catch local information. Spatial extend F exactly embodies the concept of multi-scale. F is set in range [3], [6], the step length is 0.5. Geometrical eigen-features l_λ and p_λ are set in range [0.5, 0.8], the step length is 0.1.

Fig. 13 shows the overall accuracy results of the KMAC method tested on the IQmulus and TerraMobilita Contest data-set versus the variation of spatial extent F, l_λ and p_λ, especially l_λ equals to p_λ. At the location of black point, the best classification accuracy 84.94% is gotten, and filter

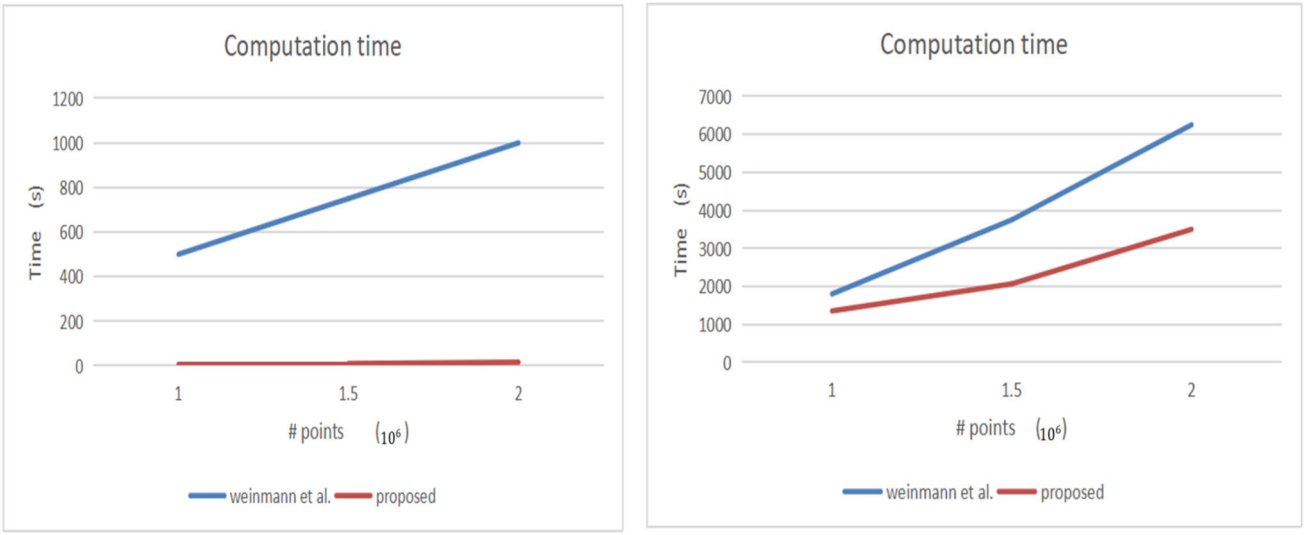

(a) (b)

FIGURE 12. The computation time comparison of the existing work by weinmann et al. [4] and the proposed method. (a) 3D block division; (b) feature extraction.

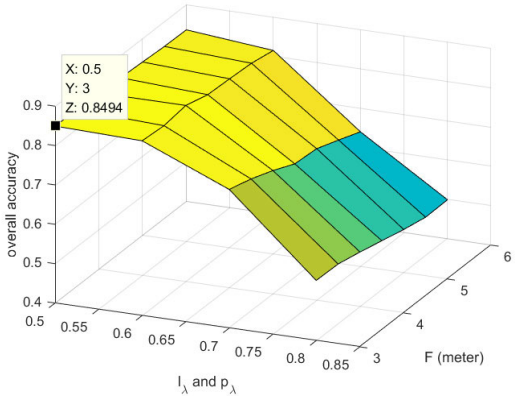

FIGURE 13. The overall accuracy (OA) results of the KMAC tested on the IQmulus and TerraMobilita Contest data-set versus the variation of spatial extent F, l_λ and p_λ.

size F equals to 3 m, both l_λ and p_λ equal to 0.5. The result demonstrates that adaptive spatial local regions of objects by convolution can be efficiently captured and the proposed method is promising to efficiently classify unlabeled objects in urban scenes.

V. CONCLUSION

In this paper, the knowledge-based multi-scale adaptive classification (KMAC) method for unlabeled urban object from MLS point clouds is proposed. The method provides ideas and guidance for unlabeled object classification in urban scenes.

Without the requirement of a large number of training samples, only basic knowledge of objects in urban scenes is needed for the proposed method. The method consisting of four layers derives from a normal neural network framework, the operation in part layers differ. As the scale difference of various objects in natural environment, multi-scale spatial local relation of objects is explored with inspiration by the idea of convolution. By extracting traditional knowledge-based features, point clouds which are adjacent with the same feature representation would be intentionally integrated into multiple 3D adaptive regions. Then, human knowledge is used to directly build an end-to-end correlation between these feature representations in 2D vectors and 3D point clouds of actual objects. The final overall accuracy on the IQmulus and TerraMobilita Contest data-set is 84.94%. The proposed method is also tested on the Paris-Rue-Madame data-set and the TUDelft Campus data-set.

Qualitative and quantitative experimental results show the proposed KMAC method is promising for unlabeled objects classification in various urban scenes. Additionally, without heavy training process, the proposed KMAC method can save a lot of the computation time.

In future work, to classify more complex classes such as pole-likes, cars, and pedestrians and so on, requires higher demand for human knowledge on different objects in urban scenes. It is necessary to define more fine features on various scales. A hierarchical decision tree is an option. In high levels, large scale is used to classify large objects such as class Trees and Facade. In low levels, one can scale down to measure small objects such as cars, pedestrians.

REFERENCES

[1] E. Özdemir, F. Remondino, and A. Golkar, "An efficient and general framework for aerial point cloud classification in urban scenarios," *Remote Sens.*, vol. 13, no. 10, p. 1985, May 2021.

[2] B. Li, "3D fully convolutional network for vehicle detection in point cloud," in *Proc. IEEE/RSJ Int. Conf. Intell. Robots Syst. (IROS)*, Sep. 2017, pp. 1513–1518.

[3] B. Yang, Z. Dong, Y. Liu, F. Liang, and Y. Wang, "Computing multiple aggregation levels and contextual features for road facilities recognition using mobile laser scanning data," *ISPRS J. Photogramm. Remote Sens.*, vol. 126, pp. 180–194, Apr. 2017.

[4] J. Xiao, M. Gerke, and G. Vosselman, "Building extraction from oblique airborne imagery based on robust façade detection," *ISPRS J. Photogramm. Remote Sens.*, vol. 68, pp. 56–68, Mar. 2012.

[5] Q. Zhu, Y. Li, H. Hu, and B. Wu, "Robust point cloud classification based on multi-level semantic relationships for urban scenes," *ISPRS J. Photogramm. Remote Sens.*, vol. 129, pp. 86–102, Jul. 2017.

[6] G. G. Pessoa et al., "Urban scene classification using features extracted from photogrammetric point clouds acquired by UAV," *Int. Arch. Photogramm., Remote Sens. Spatial Inf. Sci.*, vol. XLII-2/W13, pp. 511–518, Jun. 2019.

[7] M. Li, J. Zhang, J. Song, Z. Li, and S. Lu, "A clinical-oriented non-severe depression diagnosis method based on cognitive behavior of emotional conflict," *IEEE Trans. Computat. Social Syst.*, vol. 10, no. 1, pp. 131–141, Feb. 2023.

[8] J. Lever, M. Krzywinski, and N. Altman, "Classification evaluation," *Nature Methods*, vol. 13, no. 8, pp. 603–604, 2016.

[9] A. Agarwal, A. Beygelzimer, M. Dudík, J. Langford, and H. Wallach, "A reductions approach to fair classification," in *Proc. ICML*, Stockholm, Sweden, vol. 80, Jul. 2018, pp. 60–69.

[10] X. Zhou, X. Cai, H. Zhang, Z. Zhang, T. Jin, H. Chen, and W. Deng, "Multi-strategy competitive-cooperative co-evolutionary algorithm and its application," *Inf. Sci.*, vol. 635, pp. 328–344, Jul. 2023.

[11] Z. Ren, X. Zhen, Z. Jiang, Z. Gao, Y. Li, and W. Shi, "Underactuated control and analysis of single blade installation using a jackup installation vessel and active tugger line force control," *Mar. Struct.*, vol. 88, Mar. 2023, Art. no. 103338.

[12] H. Zhao, X. Xi, C. Wang, and F. Pan, "Ground surface recognition at voxel scale from mobile laser scanning data in urban environment," *IEEE Geosci. Remote Sens. Lett.*, vol. 17, no. 2, pp. 317–321, Feb. 2020.

[13] C. Ye, H. Zhao, L. Ma, H. Jiang, H. Li, R. Wang, M. A. Chapman, J. M. Junior, and J. Li, "Robust lane extraction from MLS point clouds towards HD maps especially in curve road," *IEEE Trans. Intell. Transp. Syst.*, vol. 23, no. 2, pp. 1505–1518, Feb. 2022.

[14] Y. Li, W. Wang, S. Tang, D. Li, Y. Wang, Z. Yuan, R. Guo, X. Li, and W. Xiu, "Localization and extraction of road poles in urban areas from mobile laser scanning data," *Remote Sens.*, vol. 11, no. 4, p. 401, Feb. 2019.

[15] J. Zhang, W. Xiao, B. Coifman, and J. P. Mills, "Vehicle tracking and speed estimation from roadside lidar," *IEEE J. Sel. Topics Appl. Earth Observ. Remote Sens.*, vol. 13, pp. 5597–5608, Sep. 2020.

[16] S. Xu and R. Wang, "Power line extraction from mobile LiDAR point clouds," *IEEE J. Sel. Topics Appl. Earth Observ. Remote Sens.*, vol. 12, no. 2, pp. 734–743, Feb. 2019.

[17] Y. Li et al., "Street tree information extraction and dynamics analysis from mobile LiDAR point cloud," *Int. Arch. Photogramm., Remote Sens. Spatial Inf. Sci.*, vol. XLIII-B2-2020, pp. 271–277, Aug. 2020.

[18] S. Xu, S. Xu, N. Ye, and F. Zhu, "Automatic extraction of street trees' non-photosynthetic components from MLS data," *Int. J. Appl. Earth Observ. Geoinf.*, vol. 69, pp. 64–77, Jul. 2018.

[19] E. Che, J. Jung, and M. Olsen, "Object recognition, segmentation, and classification of mobile laser scanning point clouds: A state of the art review," *Sensors*, vol. 19, no. 4, p. 810, Feb. 2019.

[20] A. Aijazi, A. Serna, B. Marcotegui, P. Checchin, and L. Trassoudaine, "Segmentation and classification of 3D urban point clouds: Comparison and combination of two approaches," in *Field and Service Robotics*. Cham, Switzerland: Springer, 2016, pp. 201–216.

[21] M. Soilán, L. Truong-Hong, B. Riveiro, and D. Laefer, "Automatic extraction of road features in urban environments using dense ALS data," *Int. J. Appl. Earth Observ. Geoinf.*, vol. 64, pp. 226–236, Feb. 2018.

[22] P. Babahajiani, L. Fan, and M. Gabbouj, "Object recognition in 3D point cloud of urban street scene," in *Proc. ACCV*, Singapore, Nov. 2014, pp. 177–190.

[23] M. Zheng, M. Lemmens, and P. van Oosterom, "Classification of mobile laser scanning point clouds from height features," *Int. Arch. Photogramm., Remote Sens. Spatial Inf. Sci.*, vol. XLII-2/W7, pp. 321–325, Sep. 2017.

[24] M. Zheng, M. Lemmens, and P. van Oosterom, "Classification of mobile laser scanning point clouds of urban scenes exploiting cylindrical neighbourhoods," *Int. Arch. Photogramm., Remote Sens. Spatial Inf. Sci.*, vol. 42, pp. 1225–1228, May 2018.

[25] M. Weinmann, B. Jutzi, S. Hinz, and C. Mallet, "Semantic point cloud interpretation based on optimal neighborhoods, relevant features and efficient classifiers," *ISPRS J. Photogramm. Remote Sens.*, vol. 105, pp. 286–304, Jul. 2015.

[26] M. Lehtomäki, A. Jaakkola, J. Hyyppä, J. Lampinen, H. Kaartinen, A. Kukko, E. Puttonen, and H. Hyyppä, "Object classification and recognition from mobile laser scanning point clouds in a road environment," *IEEE Trans. Geosci. Remote Sens.*, vol. 54, no. 2, pp. 1226–1239, Feb. 2016.

[27] C. R. Qi, L. Yi, H. Su, and L. J. Guibas, "PointNet++: Deep hierarchical feature learning on point sets in a metric space," in *Proc. NIPS*, Long Beach, CA, USA, Dec. 2017, pp. 5105–5114.

[28] L. Wang, Y. Huang, J. Shan, and L. He, "MSNet: Multi-scale convolutional network for point cloud classification," *Remote Sens.*, vol. 10, no. 4, p. 612, Apr. 2018.

[29] S. Pu, M. Rutzinger, G. Vosselman, and S. O. Elberink, "Recognizing basic structures from mobile laser scanning data for road inventory studies," *ISPRS J. Photogramm. Remote Sens.*, vol. 66, no. 6, pp. S28-S39, Dec. 2011.

[30] Z. Li, L. Zhang, X. Tong, B. Du, Y. Wang, L. Zhang, Z. Zhang, H. Liu, J. Mei, X. Xing, and P. T. Mathiopoulos, "A three-step approach for TLS point cloud classification," *IEEE Trans. Geosci. Remote Sens.*, vol. 54, no. 9, pp. 5412–5424, Sep. 2016.

[31] A. Aijazi, P. Checchin, and L. Trassoudaine, "Segmentation based classification of 3D urban point clouds: A super-voxel based approach with evaluation," *Remote Sens.*, vol. 5, no. 4, pp. 1624–1650, Mar. 2013.

[32] Q. Li, P. Yuan, Y. Lin, Y. Tong, and X. Liu, "Pointwise classification of mobile laser scanning point clouds of urban scenes using raw data," *J. Appl. Remote Sens.*, vol. 15, no. 2, Jun. 2021, Art. no. 024523.

[33] M. R. De Blasiis, A. Di Benedetto, and M. Fiani, "Mobile laser scanning data for the evaluation of pavement surface distress," *Remote Sens.*, vol. 12, no. 6, p. 942, Mar. 2020.

[34] J. Balado et al., "Automatic detection and characterization of ground occlusions in urban point clouds from mobile laser scanning data," *ISPRS Ann. Photogramm., Remote Sens. Spatial Inf. Sci.*, vol. VI-4/W1-2020, pp. 13–20, Sep. 2020.

[35] T. Hackel, N. Savinov, L. Ladicky, J. D. Wegner, K. Schindler, and M. Pollefeys, "Semantic3D.Net: A new large-scale point cloud classification benchmark," 2017, *arXiv:1704.03847*.

[36] J. Huang and S. You, "Point cloud labeling using 3D convolutional neural network," in *Proc. 23rd Int. Conf. Pattern Recognit. (ICPR)*, Cancun, Mexico, Dec. 2016, pp. 2670–2675.

[37] Z. Yang, W. Jiang, B. Xu, Q. Zhu, S. Jiang, and W. Huang, "A convolutional neural network-based 3D semantic labeling method for ALS point clouds," *Remote Sens.*, vol. 9, no. 9, p. 936, Sep. 2017.

[38] A. Boulch, B. Le Saux, and N. Audebert, "Unstructured point cloud semantic labeling using deep segmentation networks," in *Proc. 3DOR*, Lyon, France, vol. 2, Apr. 2017, pp. 6–7.

[39] Y. Wang, Y. Sun, Z. Liu, S. E. Sarma, M. M. Bronstein, and J. M. Solomon, "Dynamic graph CNN for learning on point clouds," 2018, *arXiv:1801.07829*.

[40] H. Thomas, C. R. Qi, J.-E. Deschaud, B. Marcotegui, F. Goulette, and L. Guibas, "KPConv: Flexible and deformable convolution for point clouds," in *Proc. IEEE/CVF Int. Conf. Comput. Vis. (ICCV)*, Seoul, South Korea, Oct. 2019, pp. 6410–6419.

[41] Y. Ma, Y. Zheng, S. Easa, Y. D. Wong, and K. El-Basyouny, "Virtual analysis of urban road visibility using mobile laser scanning data and deep learning," *Autom. Construct.*, vol. 133, Jan. 2022, Art. no. 104014.

[42] J. Balado, P. Arias, H. Lorenzo, and A. Meijide-Rodríguez, "Disturbance analysis in the classification of objects obtained from urban LiDAR point clouds with convolutional neural networks," *Remote Sens.*, vol. 13, no. 11, p. 2135, May 2021.

[43] B. Kumar, G. Pandey, B. Lohani, and S. C. Misra, "A framework for automatic classification of mobile LiDAR data using multiple regions and 3D CNN architecture," *Int. J. Remote Sens.*, vol. 41, no. 14, pp. 5588–5608, May 2020.

[44] W. Tan, N. Qin, L. Ma, Y. Li, J. Du, G. Cai, K. Yang, and J. Li, "Toronto-3D: A large-scale mobile LiDAR dataset for semantic segmentation of urban roadways," 2020, *arXiv:2003.08284*.

[45] X. Yao, J. Guo, J. Hu, and Q. Cao, "Using deep learning in semantic classification for point cloud data," *IEEE Access*, vol. 7, pp. 37121–37130, Mar. 2019.

[46] R. Zhai, X. Li, Z. Wang, S. Guo, S. Hou, Y. Hou, F. Gao, and J. Song, "Point cloud classification model based on a dual-input deep network framework," *IEEE Access*, vol. 8, pp. 55991–55999, Mar. 2020.

[47] S. Qiu, S. Anwar, and N. Barnes, "Geometric back-projection network for point cloud classification," *IEEE Trans. Multimedia*, vol. 24, pp. 1943–1955, 2022.

[48] W. H. Bangyal, J. Ahmad, I. Shafi, and Q. Abbas, "A forward only counter propagation network-based approach for contraceptive method choice classification task," *J. Exp. Theor. Artif. Intell.*, vol. 24, no. 2, pp. 211–218, Jun. 2012.

[49] S. Pervaiz, Z. Ul-Qayyum, W. H. Bangyal, L. Gao, and J. Ahmad, "A systematic literature review on particle swarm optimization techniques for medical diseases detection," *Comput. Math. Methods Med.*, vol. 2021, pp. 1–10, Sep. 2021.

[50] S. Hershey, S. Chaudhuri, D. P. W. Ellis, J. F. Gemmeke, A. Jansen, R. C. Moore, M. Plakal, D. Platt, R. A. Saurous, B. Seybold, M. Slaney, R. J. Weiss, and K. Wilson, "CNN architectures for large-scale audio classification," 2016, *arXiv:1609.09430*.

[51] Q. Sun, M. Zhang, L. Zhou, K. Garme, and M. Burman, "A machine learning-based method for prediction of ship performance in ice: Part I. Ice resistance," *Mar. Struct.*, vol. 83, May 2022, Art. no. 103181.

[52] M. Li, W. Zhang, B. Hu, J. Kang, Y. Wang, and S. Lu, "Automatic assessment of depression and anxiety through encoding pupil-wave from HCI in VR scenes," *ACM Trans. Multimedia Comput., Commun., Appl.*, vol. 20, no. 2, pp. 1–22, Feb. 2024.

[53] W. H. Bangyal, K. Nisar, A. A. B. A. Ibrahim, M. R. Haque, J. J. P. C. Rodrigues, and D. B. Rawat, "Comparative analysis of low discrepancy sequence-based initialization approaches using population-based algorithms for solving the global optimization problems," *Appl. Sci.*, vol. 11, no. 16, p. 7591, Aug. 2021.

[54] W. H. Bangyal, J. Ahmad, and Q. Abbas, "Recognition of off-line isolated handwritten character using counter propagation network," *Int. J. Eng. Technol.*, vol. 5, no. 2, pp. 227–230, Jan. 2013.

[55] T. Hackel, J. D. Wegner, and K. Schindler, "Fast semantic segmentation of 3D point clouds with strongly varying density," *ISPRS Ann. Photogramm., Remote Sens. Spatial Inf. Sci.*, vol. III-3, pp. 177–184, Jun. 2016.

[56] T. Hackel, J. D. Wegner, and K. Schindler, "Joint classification and contour extraction of large 3D point clouds," *ISPRS J. Photogramm. Remote Sens.*, vol. 130, pp. 231–245, Aug. 2017.

[57] M. Weinmann, B. Jutzi, S. Hinz, and C. Mallet, "Semantic point cloud interpretation based on optimal neighborhoods, relevant features and efficient classifiers," *ISPRS J. Photogramm. Remote Sens.*, vol. 105, pp. 286–304, Jul. 2015.

[58] M. Weinmann et al., "Geometric features and their relevance for 3D point cloud classification," *ISPRS Ann. Photogramm., Remote Sens. Spatial Inf. Sci.*, vol. IV-1/W1, pp. 157–164, May 2017.

[59] J. Demantké et al., "Dimensionality based scale selection in 3D LiDAR point clouds," *Int. Arch. Photogramm., Remote Sens. Spatial Inf. Sci.*, vol. XXXVIII-5/W12, pp. 97–102, Sep. 2012.

[60] M. Gunst, "Automatic extraction of roads from SPOT images," Fac. Geodesy, TU Delft, Delft, The Netherlands, Jan. 1991.

[61] M. Gunst and M. Lemmens, "Automatized updating of road databases from scanned aerial photographs," *Int. Arch. Photogramm. Remote Sens. Spat. Inf. Sci.*, vol. 29, pp. 477–484, May 1992.

[62] G. Vosselman and M. Gunst, "Updating road maps by contextual reasoning," in *Automatic Extraction of Man-Made Objects from Aerial and Space Images (II)*, A. Gruen, E. P. Baltsavias and O. Henricsson, Eds. Basel, Switzerland: Birkhäuser Verlag, 1997, pp. 267–276.

[63] C. Zhang and E. Baltsavias, "Knowledge-based image analysis for 3D edge extraction and road reconstruction," *Int. Arch. Photogramm. Remote Sens. Spat. Inf. Sci.*, vol. 33, no. Part B3/2, pp. 1008–1015, 2000.

[64] M. Lemmens, "On a knowledge-based approach to the classification of mobile laser scanning point clouds," *Int. Arch. Photogramm., Remote Sens. Spatial Inf. Sci.*, vol. XLII-4, pp. 343–349, Sep. 2018.

[65] M. Zheng and H. Wu, "Vehicle recognition based on region growth of relative tension and similarity measurement of side projection profile of vehicle body," *Remote Sens.*, vol. 15, no. 6, p. 1493, Mar. 2023.

[66] C. Zhao, H. Guo, J. Lu, D. Yu, D. Li, and X. Chen, "ALS point cloud classification with small training data set based on transfer learning," *IEEE Geosci. Remote Sens. Lett.*, vol. 17, no. 8, pp. 1406–1410, Aug. 2020.

[67] X. Hu and Y. Yuan, "Deep-learning-based classification for DTM extraction from ALS point cloud," *Remote Sens.*, vol. 8, no. 9, p. 730, Sep. 2016.

[68] B. Vallet, M. Brédif, A. Serna, B. Marcotegui, and N. Paparoditis, "TerraMobilita/iQmulus urban point cloud analysis benchmark," *Comput. Graph.*, vol. 49, pp. 126–133, Jun. 2015.

[69] A. Serna, B. Marcotegui, F. Goulette, and J.-E. Deschaud, "Paris-rue-Madame database: A 3D mobile laser scanner dataset for benchmarking urban detection, segmentation and classification methods," in *Proc. 4th Int. Conf. Pattern Recognit. Appl. Methods*, Angers, France, Mar. 2014, pp. 819–824.

[70] W. Zhang, J. Qi, P. Wan, H. Wang, D. Xie, X. Wang, and G. Yan, "An Easy-to-Use airborne LiDAR data filtering method based on cloth simulation," *Remote Sens.*, vol. 8, no. 6, p. 501, Jun. 2016.

[71] D. Girardeau-Montaut, *Cloud Compare*. Paris, France: Électricité de France, S.A., Ed.; (EDF) R&D, 2003.

[72] M. Zheng, H. Wu, and Y. Li, "An adaptive end-to-end classification approach for mobile laser scanning point clouds based on knowledge in urban scenes," *Remote Sens.*, vol. 11, no. 2, p. 186, Jan. 2019.

[73] H. Gross and U. Thoennessen, "Extraction of lines from laser point clouds," *Int. Arch. Photogramm. Remote Sens. Spat. Inf. Sci.*, vol. 36, pp. 86–89, Sep. 20061.

[74] J. Demantké et al., "Dimensionality based scale selection in 3D LiDAR point clouds," *Int. Arch. Photogramm., Remote Sens. Spatial Inf. Sci.*, vol. XXXVIII-5/W12, pp. 97–102, Sep. 2012.

[75] C.-H. Lin, J.-Y. Chen, P.-L. Su, and C.-H. Chen, "Eigen-feature analysis of weighted covariance matrices for LiDAR point cloud classification," *ISPRS J. Photogramm. Remote Sens.*, vol. 94, pp. 70–79, Aug. 2014.

[76] W. R. Tobler, "A computer movie simulating urban growth in the Detroit region," *Econ. Geography*, vol. 46, pp. 234–240, Jun. 1970.

[77] E. Schubert, J. Sander, M. Ester, H. P. Kriegel, and X. Xu, "DBSCAN revisited, revisited: Why and how you should (Still) use DBSCAN," *ACM Trans. Database Syst.*, vol. 42, no. 3, pp. 1–21, Jul. 2017.

[78] J. A. Hartigan and M. A. Wong, "A K-means clustering algorithm," *Appl. Stat.*, vol. 28, no. 1, pp. 100–108, 1979.

[79] D. Comaniciu and P. Meer, "Mean shift analysis and applications," in *Proc. 7th IEEE Int. Conf. Comput. Vis.*, Kerkyra, Greece, Sep. 1999, pp. 20–27.

[80] J. West, D. Ventura, and S. Warnick, "Spring research presentation: A theoretical foundation for inductive transfer," College Phys. Math. Sci., Brigham Young Univ., Provo, UT, USA, 2007, vol. 1.

[81] S. J. Pan and Q. Yang, "A survey on transfer learning," *IEEE Trans. Knowl. Data Eng.*, vol. 22, no. 10, pp. 1345–1359, Jan. 2021.

[82] S. Thrun and L. Pratt, *Learning to Learn*. USA: Springer, 2012.

[83] Q. Yang, Y. Zhang, W. Dai, and J. Pan, *Transfer Learning*. Cambridge Univ. Press, 2020.

[84] M. Weinmann, S. Urban, S. Hinz, B. Jutzi, and C. Mallet, "Distinctive 2D and 3D features for automated large-scale scene analysis in urban areas," *Comput. Graph.*, vol. 49, pp. 47–57, Jun. 2015.

MINGXUE ZHENG received the M.S. degree in applied mathematics and the Ph.D. degree in cartography and geographical information engineering from Wuhan University, in 2015 and 2020, respectively. She is currently an Assistant Researcher with the Hubei Academy of Agricultural Sciences. Her research interests include deep learning and object recognition and classification.

XIANGCHENG SHEN received the B.S. degree in agricultural economics from the Zhongnan University of Economics and Law, in 1989. He is currently a Research Fellow with the Hubei Academy of Agricultural Sciences. His research interests include agricultural informatization and big data mining.

ZHIQING LUO received the M.S. degree in computer application technology and the Ph.D. degree in geoinformatics engineering from the China University of Geosciences, in 2007 and 2012, respectively. He is currently an Associate Researcher with the Hubei Academy of Agricultural Sciences. He is mainly involved in research on pattern recognition and 3-D modeling on smart agriculture.

PINGTING CHEN received the master's degree in landscape architecture and the Ph.D. degree in landscape plant and ornamental horticulture from Huazhong Agricultural University, in 2005 and 2011, respectively. She is currently an Associate Researcher with the Hubei Academy of Agricultural Sciences. Her research interest includes agricultural informatization.

BO GUAN received the master's degree in library and information from Central China Normal University, Wuhan, in 2010, and the Ph.D. degree in agricultural economics from the Zhongnan University of Economics and Law, in 2014. He is currently an Assistant Researcher with the Hubei Academy of Agricultural Sciences. His research interest includes agricultural and rural informatization.

JICHENG YI received the master's degree in applied statistics from the Yunnan University of Finance and Economics, Yunnan, in 2017, and the Ph.D. degree from the Zhongnan University of Economics and Law, in 2021. He is currently a Postdoctoral Researcher with the Institute of Agricultural Economy and Technology, Hubei Academy of Agricultural Sciences. His research interest includes digital development mechanism and evaluation.

HAIRONG MA was born in Shandong, China. She received the B.S., M.S., and Ph.D. degrees in geomatics and remote sensing from the China University of Geosciences, in 2011, 2013, and 2016, respectively. She is currently an Assistant Researcher with the Hubei Academy of Agricultural Sciences. Her research interests include data mining, object recognition, and digital image classification.